

Production of Z^0 bosons with rapidity gaps: Exclusive photoproduction in γp and pp collisions and inclusive double diffractive Z^0 's

A. Cisek,^{1,*} W. Schäfer,^{1,†} and A. Szczurek^{1,2,‡}

¹*Institute of Nuclear Physics PAN, PL-31-342 Cracow, Poland*

²*University of Rzeszów, PL-35-959 Rzeszów, Poland*

(Received 9 June 2009; published 14 October 2009)

We extend the k_{\perp} -factorization formalism for exclusive photoproduction of vector mesons to the production of electroweak Z^0 bosons. Predictions for the $\gamma p \rightarrow Z^0 p$ and $pp \rightarrow ppZ^0$ reactions are given using an unintegrated gluon distribution tested against deep inelastic data. We show distributions in the Z^0 rapidity, transverse momentum of Z^0 as well as in relative azimuthal angle between outgoing protons. The contributions of different flavors are discussed. Absorption effects lower the cross section by a factor of 1.5–2, depending on the Z -boson rapidity. We also discuss the production of Z^0 bosons in central inclusive production. Here rapidity and $(x_{\mathbb{P},1}, x_{\mathbb{P},2})$ distributions of Z^0 are calculated. The corresponding cross section is about 3 orders of magnitude larger than that for the purely exclusive process.

DOI: 10.1103/PhysRevD.80.074013

PACS numbers: 12.38.–t, 12.38.Bx, 14.70.Hp

I. INTRODUCTION

Recently there has been much experimental progress in the field of central exclusive production. The observation of exclusive central dijets [1], as well as charmonia/ $\mu^+ \mu^-$ -pairs [2], has clearly demonstrated the feasibility of detecting exclusive final states at collider energies. These are good prospects for possible future studies at the LHC, addressing a wide range of physics problems, from Higgs physics to the investigations of the QCD-Pomeron and hadronic structure of the produced particles. For recent reviews see for example [3] for theory/phenomenology, and [4] for experiment.

The mechanism of the reaction strongly depends on the centrally produced particle, in particular, its spin, parity, C-parity and internal structure. For heavy vector quarkonia such as J/Ψ and Υ the photon-Pomeron fusion is the dominant mechanism (for recent calculations see e.g. [5,6]). The same is expected for the Z^0 gauge boson [7,8]. The dominant reaction mechanism is shown in Fig. 1.

Here, the essential ingredient is the $\gamma p \rightarrow Z^0 p$ subprocess, which proceeds through the $q\bar{q}$ component of the virtual photon. There is a strong similarity to the production of $q\bar{q}$ vector mesons, and one would expect the QCD description of this process to follow from the color dipole/ k_{\perp} -factorization approach to vector-meson production (for a review, see [9]) by straightforward modifications [7,8]. The important distinction to the case of vector-meson production is the fact that the $q\bar{q}$ pair coupling to the Z^0 -boson can be put on its mass-shell. In the impact-parameter space color-dipole formulation, this requires us to continue the light-cone wave function of the Z^0 to

the region of complex arguments. The resulting highly oscillatory integrands are however not straightforward to handle [8].

In the momentum space representation given in this work, the situation is more transparent, and the numerics poses no special problems.

Previous calculations of the $pp \rightarrow ppZ^0$ process made use of the equivalent-photon approximation (EPA) and did not include absorption effects. In the EPA only total cross section or rapidity distribution of the Z^0 boson can be calculated. In this paper we use the formalism of [5,6] to perform the calculation at the amplitude-level, which al-

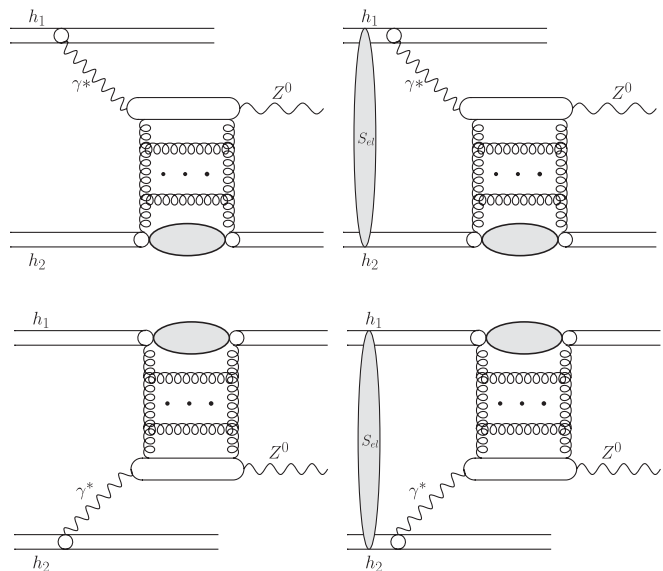


FIG. 1. Diagrammatic representation of the photon-Pomeron (top) and Pomeron-photon (bottom) mechanisms of exclusive Z^0 -boson production in hadronic collisions. The left row depicts the Born-level amplitudes, while in the right row absorptive corrections are included.

*Anna.Cisek@ifj.edu.pl

†Wolfgang.Schafer@ifj.edu.pl

‡Antoni.Szczurek@ifj.edu.pl

lows us to calculate other differential observables (e.g. in Z^0 boson transverse momentum or correlation in relative azimuthal angle between outgoing protons) and to include absorption corrections.

The cross sections for exclusive Z^0 production for both the Tevatron and LHC are very small. In fact a recent search for exclusive Z^0 [10] only puts rather generous bounds on the cross section. The exclusive events are characterized by large rapidity gaps between centrally produced Z^0 bosons and very forward or very backward final state nucleons. Another process with these features is the inclusive double-diffractive production of Z^0 , which to our knowledge was not previously calculated in the literature.¹ In the latter case the Z^0 in the central rapidity region is associated with low-multiplicity hadronic activity.

II. $\gamma p \rightarrow Z^0 p$ PHOTOPRODUCTION PROCESS

Before we go to the hadronic reaction let us start from the real photoproduction process depicted in Fig. 2. The forward production amplitude can be written very much the same way as for exclusive photoproduction of vector quarkonia (see for example [9]):

$$\mathcal{M}(W, \Delta^2 = 0) = W^2 \sum_f \frac{4\pi\alpha g_V^f}{4\pi^2} 2 \int_0^1 dz \int d^2k \times \frac{\mathcal{A}_f(z, \mathbf{k}^2)}{\mathbf{k}^2 + m_f^2 - z(1-z)M_Z^2 - i\epsilon}. \quad (2.1)$$

As was already shown in [7,8], only the vectorial part of the $Z^0 q\bar{q}$ -coupling contributes to the forward amplitude,

$$g_V^f = \frac{I_{3f} - 2e_f \sin^2 \Theta_W}{\sin 2\Theta_W} \quad (2.2)$$

is the relevant weak vector coupling, I_{3f} is the weak isospin of a quark of flavor f , e_f is its charge, and Θ_W is the Weinberg angle. The imaginary part of \mathcal{A}_f can be obtained from the results given for vector-meson production with the γ_μ vertex in [9]. Performing azimuthal integrals one obtains [6]:

$$\Im m \mathcal{A}_f(z, \mathbf{k}^2) = \pi \int_0^\infty \frac{\pi d\kappa^2}{\kappa^4} \alpha_s(q^2) \mathcal{F}(x, \kappa^2) \times (A_{0f}(z, k^2) W_{0f}(k^2, \kappa^2) + A_{1f}(z, k^2) W_{1f}(k^2, \kappa^2)) \quad (2.3)$$

with

$$A_{0f}(z, k^2) = m_f^2, \\ A_{1f}(z, k^2) = [z^2 + (1-z)^2] \frac{k^2}{k^2 + m_f^2},$$

¹So far only the single-diffractive contribution was estimated in the literature, see e.g. [11].

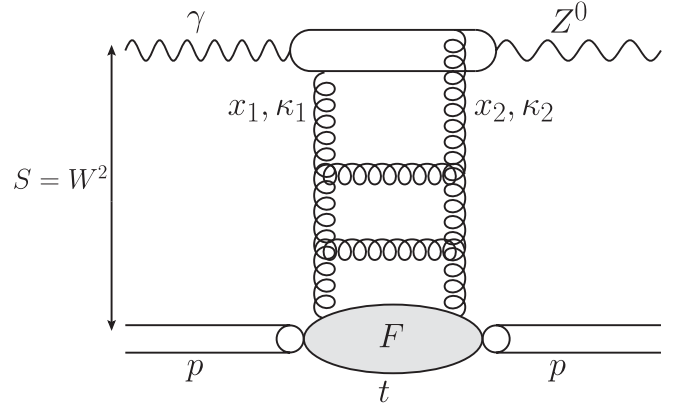


FIG. 2. A pQCD diagram for the $\gamma p \rightarrow Z^0 p$ amplitude at large γp cm-energy. The gluon exchange ladder is modeled by the unintegrated gluon distribution of the target.

and

$$W_{0f}(k^2, \kappa^2) = \frac{1}{k^2 + m_f^2} - \frac{1}{\sqrt{(k^2 - m_f^2 - \kappa^2)^2 + 4m_f^2 k^2}}, \\ W_{1f}(k^2, \kappa^2) = 1 - \frac{k^2 + m_f^2}{2k^2} \times \left(1 + \frac{k^2 - m_f^2 - \kappa^2}{\sqrt{(k^2 - m_f^2 - \kappa^2)^2 + 4m_f^2 k^2}} \right).$$

The strong coupling α_s enters at the scale $q^2 = \max\{k^2 + m_f^2, \kappa^2\}$. The unintegrated gluon distribution $\mathcal{F}(x, \kappa^2)$ is sampled at $x = c_{\text{skewed}} \cdot M_Z^2/W^2$ with $c_{\text{skewed}} = 0.41$. This shifted value of x simulates the prescription of [12] to obtain the skewed distribution from the diagonal one, and is valid for the particular gluon distribution we use [9]. Now, let

$$z_{\pm} = \frac{1}{2} \left(1 \pm \sqrt{1 - \frac{4m_f^2}{M_Z^2}} \right), \quad (2.4)$$

then, the integration domain $z \in [0, 1]$ must be split into $[0, z_-] \cup [z_-, z_+] \cup [z_+, 1]$. Apparently, within the subdomain $[z_-, z_+]$ the denominator in Eq. (2.1) can go to zero, which means that the $q\bar{q}$ state after the interaction can go on-shell. This leads to a rotation of the complex phase of the dominantly imaginary amplitude. For $z \in [z_-, z_+]$, one must use the Plemelj-Sokhocki formula

$$\frac{1}{\mathbf{k}^2 + m_f^2 - z(1-z)M_Z^2 - i\epsilon} = \text{PV} \frac{1}{\mathbf{k}^2 + m_f^2 - z(1-z)M_Z^2} + i\pi\delta(\mathbf{k}^2 + m_f^2 - z(1-z)M_Z^2), \quad (2.5)$$

where PV denotes the principal value integral. It can be evaluated as

$$\begin{aligned}
 \text{PV} \int_0^\infty dk^2 \frac{\mathcal{A}_f(z, k^2)}{k^2 - \tau^2} \\
 = \int_0^{(1+\lambda)\tau^2} dk^2 \frac{\mathcal{A}_f(z, k^2) - \mathcal{A}_f(z, \tau^2)}{k^2 - \tau^2} \\
 + \int_{(1+\lambda)\tau^2}^\infty dk^2 \frac{\mathcal{A}_f(z, k^2)}{k^2 - \tau^2} + \mathcal{A}_f(z, \tau^2) \log(\lambda), \quad (2.6)
 \end{aligned}$$

for an arbitrary positive value of λ . Here $\tau^2 = z(1-z)M_Z^2 - m_f^2$ is positive in the relevant integration domain.

Another distinction in comparison to the vector-meson (VM) photoproduction is worth a comment. Effectively, we replace the nonperturbative light-cone wave function of the VM by the propagator:

$$\psi_V(z, \mathbf{k}^2) \rightarrow \frac{1}{\mathbf{k}^2 + m_f^2 - z(1-z)M_Z^2 - i\epsilon}. \quad (2.7)$$

While in the case of vector-mesons, the light-cone wave function will suppress the endpoint-region $z, 1-z \ll 1$, no such suppression of asymmetric $q\bar{q}$ pairs is available here. Incidentally, in impact-parameter space asymmetric pairs correspond to large dipole sizes [13], and it is precisely the wave-function suppression of large dipoles which leads to the dipole-size scanning property [9,14] of VM production amplitudes. Therefore, strictly speaking, the Z^0 production cross section is not purely perturbatively calculable, but one must rely on the ability of the color-dipole/ k_\perp -factorization approaches to properly factorize the large dipole/infrared contributions. Compare this to the *scaling* contribution of large dipoles to the transverse deep inelastic scattering (DIS) structure function $F_T(x, Q^2) = 2xF_1(x, Q^2)$ [13,15] at large Q^2 .

Finally, we note, that we restore the real part of the amplitude by substituting

$$\mathcal{A}_f = (i + \rho) \Im m \mathcal{A}_f, \quad (2.8)$$

where $\rho = \tan(\pi\Delta_{\mathbf{IP}}/2)$, and $\Delta_{\mathbf{IP}} = \partial \log \Im m \mathcal{A}_f / \partial \log W^2$, and the $\gamma p \rightarrow Z^0 p$ amplitude within the diffraction cone is given by

$$\mathcal{M}(W^2, \Delta^2) = \mathcal{M}(W^2, \Delta^2 = 0) \exp[Bt], \quad (2.9)$$

where $t = -\Delta^2$ and the running diffraction slope is taken as

$$B = B_0 + 2\alpha'_{\text{eff}} \log(W^2/W_0^2), \quad (2.10)$$

with $\alpha'_{\text{eff}} = 0.164 \text{ GeV}^{-2}$ [16], and $B_0 = 3.5 \text{ GeV}^{-2}$, $W_0 = 95 \text{ GeV}$.

In general, the slope for a diffractive process receives contributions from the proton vertex, the Pomeron exchange (through α'), and from the $\gamma \rightarrow V$ transition vertex. In vector-meson photoproduction, what matters is the dipole scanning radius r_S , and the contribution from the transition vertex to the diffraction slope will be propor-

tional to r_S^2 (see [9] and references therein). As we stressed above, there is no scanning radius in the Z^0 production, because of the pointlike Z^0 -coupling.

We chose $B_0 = 3.5 \text{ GeV}^{-2}$, as a much smaller value would arguably question our understanding of the proton size. The rather smallish value of B_0 favors a larger production cross section, and does not introduce additional suppression ‘‘by hand.’’

Finally, the total cross section for $\gamma p \rightarrow Zp$ is given by

$$\sigma_{\text{tot}}(\gamma p \rightarrow Zp; W) = \frac{1}{16\pi B} |\mathcal{M}(W^2, 0)|^2. \quad (2.11)$$

III. $pp \rightarrow ppZ^0$ EXCLUSIVE HADROPRODUCTION

Assuming only helicity conserving processes the Born amplitude for the $pp \rightarrow ppZ^0$ reaction is a sum of amplitudes of the processes shown in the left row of Fig. 1 and can be written through the amplitudes of photoproduction processes $\gamma h_2 \rightarrow Z^0 h_2$ or $\gamma h_2 \rightarrow Z^0 h_2$, discussed above, in the form of the vector

$$\begin{aligned}
 \mathbf{M}_{h_1 h_2 \rightarrow h_1 h_2 Z^0}^{(0)}(\mathbf{p}_1, \mathbf{p}_2) = e_1 \sqrt{4\pi\alpha_{em}} F_1(t_1) \frac{2\mathbf{p}_1}{z_1 t_1} \\
 \cdot \mathcal{M}_{\gamma^* h_2 \rightarrow Z^0 h_2}(Q_1^2, s_2, t_2) \\
 + e_2 \sqrt{4\pi\alpha_{em}} F_1(t_2) \frac{2\mathbf{p}_2}{z_2 t_2} \\
 \cdot \mathcal{M}_{\gamma^* h_1 \rightarrow Z^0 h_1}(Q_2^2, s_1, t_1). \quad (3.1)
 \end{aligned}$$

Above $Q_1^2 = -t_1$ and $Q_2^2 = -t_2$ are virtualities of photons, F_1 is the familiar Dirac electromagnetic form factor of the proton/antiproton and $\mathbf{p}_1, \mathbf{p}_2$ are transverse momenta of outgoing protons. In the present analysis we shall use a simple parametrization of the Dirac electromagnetic form factor F_1 taken from Ref. [17].

The dependence of the virtual photoproduction subprocess amplitude on spacelike virtuality of the photon Q^2 is in practice entirely negligible (recall that $Q^2 \ll M_Z^2$). Furthermore, we checked numerically that in the $\gamma p \rightarrow Zp$ process $\sigma_L/\sigma_T \ll 1$, so that the contribution from longitudinal photons can be safely neglected.

In the hadroproduction process one has to include additional absorption corrections. The relevant formalism for the calculation of amplitudes and cross sections was reviewed in some detail in Ref. [5]. Here we give only a the main formulas. The basic mechanisms are shown in the right row of Fig. 1.

Inclusion of absorptive corrections (the ‘‘elastic rescattering’’) leads in momentum space to the full, absorbed amplitude

$$\begin{aligned}
 \mathbf{M}(\mathbf{p}_1, \mathbf{p}_2) = \int \frac{d^2\mathbf{k}}{(2\pi)^2} S_{\text{el}}(\mathbf{k}) \mathbf{M}^{(0)}(\mathbf{p}_1 - \mathbf{k}, \mathbf{p}_2 + \mathbf{k}) \\
 = \mathbf{M}^{(0)}(\mathbf{p}_1, \mathbf{p}_2) - \delta \mathbf{M}(\mathbf{p}_1, \mathbf{p}_2). \quad (3.2)
 \end{aligned}$$

With

$$S_{\text{el}}(\mathbf{k}) = (2\pi)^2 \delta^{(2)}(\mathbf{k}) - \frac{1}{2} T(\mathbf{k}),$$

$$T(\mathbf{k}) = \sigma_{\text{tot}}^{p\bar{p}}(s) \exp\left(-\frac{1}{2} B_{\text{el}} k^2\right), \quad (3.3)$$

where at Tevatron energy $\sqrt{s} = 1800$ GeV $\sigma_{\text{tot}}^{p\bar{p}}(s) = 76$ mb, $B_{\text{el}} = 17$ GeV $^{-2}$ [18], the absorptive correction δM reads

$$\delta M(\mathbf{p}_1, \mathbf{p}_2) = \int \frac{d^2 \mathbf{k}}{2(2\pi)^2} T(\mathbf{k}) M^{(0)}(\mathbf{p}_1 - \mathbf{k}, \mathbf{p}_2 + \mathbf{k}). \quad (3.4)$$

The differential cross section is given in terms of M as

$$d\sigma = \frac{1}{512\pi^4 s^2} |M|^2 dy dt_1 dt_2 d\phi, \quad (3.5)$$

where y is the rapidity of the Z^0 -boson, t_1, t_2 are four-momentum transfers squared, and ϕ is the angle between transverse momenta \mathbf{p}_1 and \mathbf{p}_2 .

IV. INCLUSIVE DOUBLE DIFFRACTIVE PRODUCTION OF Z^0

The purely exclusive process discussed so far can be characterized by large rapidity gaps between the centrally produced Z^0 and forward/backward emitted protons/antiprotons. Can the rapidity gap method be used to identify this process? The discussed exclusive process is not the only one with double rapidity gaps. The inclusive double-Pomeron cross section for Z^0 boson production was apparently not previously calculated. The mechanism is depicted in Fig. 3.

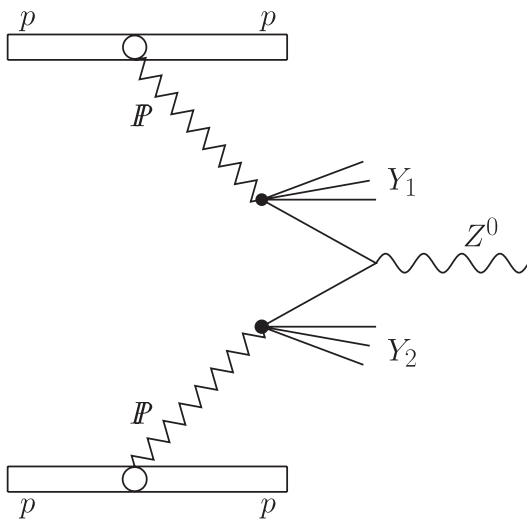


FIG. 3. Pomeron-Pomeron fusion representation of the central diffractive inclusive Z^0 production. The hard subprocess is viewed as a collision of partons of the Pomeron.

Following Ingelman and Schlein [19], one may try to estimate the hard diffractive process by assuming that the Pomeron has a well defined partonic structure, and that the hard process takes place in a Pomeron-Pomeron collision. Then the rapidity distribution of Z^0 -bosons would be obtained from

$$\frac{d\sigma(pp \rightarrow ppZ^0X)}{dy} = K \sum_f \sigma(q_f \bar{q}_f \rightarrow Z^0; x_1 x_2 s) (x_1 q_f^D(x_1, \mu^2) x_2 \bar{q}_f^D(x_2, \mu^2) + (1 \leftrightarrow 2)). \quad (4.1)$$

Here

$$x_1 = \frac{M_Z}{\sqrt{s}} e^y, \quad x_2 = \frac{M_Z}{\sqrt{s}} e^{-y},$$

$\sigma_{q_f \bar{q}_f \rightarrow Z^0}(\hat{s})$ is the elementary “zeroth-order” flavor-dependent cross sections (see e.g. [20]). K in Eq. (4.1) stands for the Drell-Yan type K -factor which includes approximately pQCD NLO corrections [20].

The effective “diffractive” quark distribution of flavor f is given by a convolution of the flux of Pomerons $f_{\mathbf{IP}}(x_{\mathbf{IP}})$ and the parton distribution in a Pomeron $q_{f/\mathbf{IP}}(\beta, \mu^2)$:

$$q_f^D(x_1, \mu^2) = \int dx_{\mathbf{IP}} d\beta \delta(x - x_{\mathbf{IP}} \beta) q_{f/\mathbf{IP}}(\beta, \mu^2) f_{\mathbf{IP}}(x_{\mathbf{IP}}) = \int_x^1 \frac{dx_{\mathbf{IP}}}{x_{\mathbf{IP}}} f_{\mathbf{IP}}(x_{\mathbf{IP}}) q_{f/\mathbf{IP}}\left(\frac{x}{x_{\mathbf{IP}}}, \mu^2\right). \quad (4.2)$$

The flux of Pomerons $f_{\mathbf{IP}}(x_{\mathbf{IP}})$ enters in the form integrated over four-momentum transfer

$$f_{\mathbf{IP}}(x_{\mathbf{IP}}) = \int_{t_{\min}}^{t_{\max}} dt f(x_{\mathbf{IP}}, t), \quad (4.3)$$

with t_{\min}, t_{\max} being the kinematic boundaries.

Both Pomeron-flux factors $f_{\mathbf{IP}}(x_{\mathbf{IP}}, t)$ as well as quark/antiquark distributions in the Pomeron were taken from the H1 Collaboration analysis of diffractive structure function and/or from the analysis of diffractive dijets at HERA [21]. The factorization scale is taken as $\mu_F^2 = M_Z^2$.

Besides the Pomeron-exchange, one must also include the secondary Reggeon-exchange contribution, which dominates at larger $x_{\mathbf{IP}}$. Consequently, a number of interference contributions arise, which are shown diagrammatically in Fig. 4. As we wish to use the results of the H1 analysis of diffractive DIS at HERA, we have to omit a number of interference terms, which would involve Reggeon-Pomeron interference structure functions that have been neglected in the H1 analysis. Incidentally, within pQCD, there is no reason why interference terms should be small, and in fact, they enter the diffractive structure functions in the maximal possible way [22]. While one obtains good fits of HERA data, even omitting the $\mathbf{IR} - \mathbf{IP}$ interference, the rather unphysical values of the so-extracted Reggeon trajectory parameters show the limita-

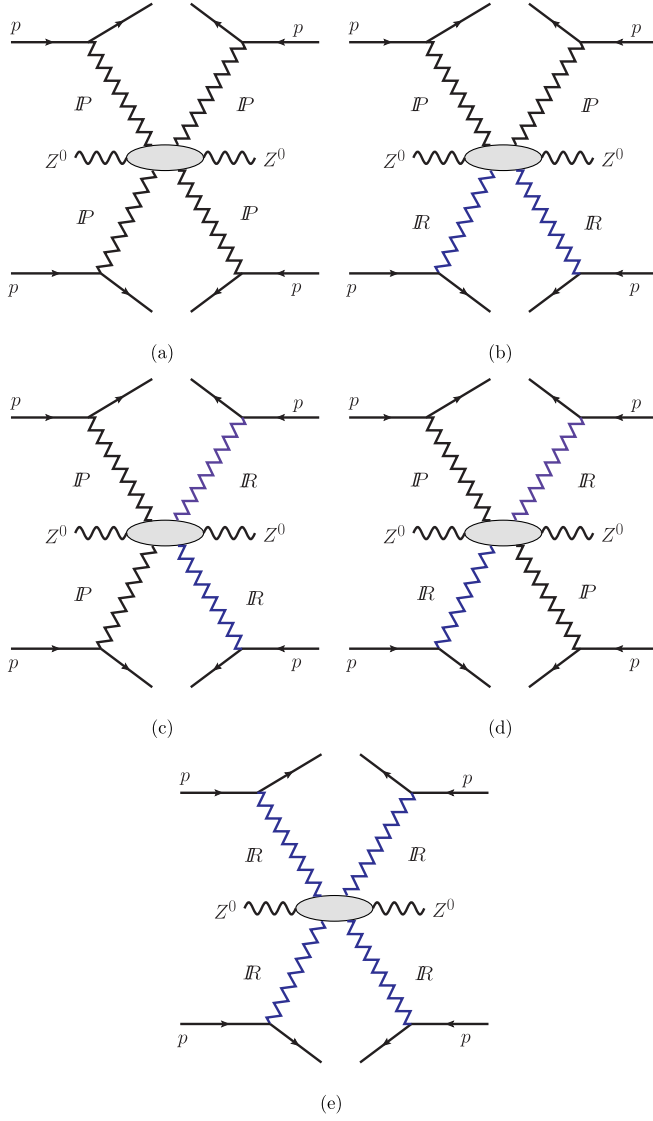


FIG. 4 (color online). Mueller-Kancheli diagrams for the process $pp \rightarrow p + \text{gap} + Z^0 X + \text{gap} + p$. Interference diagrams of type (c, d), which would involve $\mathbf{IP} - \mathbf{IR}$ interference structure functions are neglected.

tions of such a procedure. Clearly though, a full reanalysis of H1 data is not warranted for our purpose of obtaining a first estimate of the Z^0 -production cross section.

It is however obvious that the naive factorization prescription of Eq. (4.1) cannot be correct. It neglects rescattering effects of incoming protons shown in Fig. 5. Indeed such diagrams quantify the probability that protons emerge intact out of the interaction region in a regime where the typical events are highly inelastic and many channels are open [23]. Here we restrict ourselves to only a “minimal” scenario of factorization breaking induced by eikonized multiple scatterings, following the formalism of Ref. [24] (for a somewhat modernized version, see [25]).

We do not enter here the debate on the possible relevance of multiple-Pomeron vertices (see, for example, the

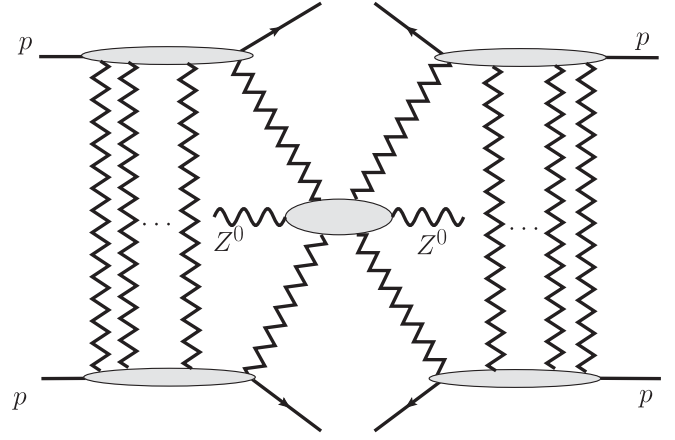


FIG. 5. Absorptive correction to the \mathbf{IP} -exchange contribution.

reviews [3,26] and references therein), but keep in mind that our treatment of absorption may require a revision after better knowledge on soft interactions at the LHC has been acquired.

The relevant formulas are most easily written in impact-parameter space. As in practice $t_i \sim -\mathbf{q}_i^2$, where \mathbf{q}_i is the transverse momentum transfer to proton i , we can write

$$f_{\mathbf{IP}}(x_{\mathbf{IP}}, t) = f_{\mathbf{IP}}(x_{\mathbf{IP}}, \mathbf{q}) = f_{\mathbf{IP}}(x_{\mathbf{IP}}) \exp[-B\mathbf{q}^2], \quad (4.4)$$

where $B = B(x_{\mathbf{IP}}) = B_D + 2\alpha'_{\mathbf{IP}} \log(1/x_{\mathbf{IP}})$ is the $x_{\mathbf{IP}}$ -dependent diffractive slope. We follow the H1-analysis [21], and use the central values of their fit $B_D = 5.5 \text{ GeV}^{-2}$, $\alpha'_{\mathbf{IP}} = 0.06 \text{ GeV}^{-2}$. Then, in impact-parameter space, we have

$$\begin{aligned} f_{\mathbf{IP}}(x_{\mathbf{IP}}, \mathbf{b}) &= \int \frac{d^2\mathbf{q}}{(2\pi)^2} f_{\mathbf{IP}}(x_{\mathbf{IP}}, \mathbf{q}) \exp[-i\mathbf{b}\mathbf{q}] \\ &= \frac{f_{\mathbf{IP}}(x_{\mathbf{IP}})}{4\pi B} \exp\left[-\frac{\mathbf{b}^2}{4B}\right] \equiv f_{\mathbf{IP}}(x_{\mathbf{IP}}) t_{\mathbf{IP}}(x_{\mathbf{IP}}, \mathbf{b}). \end{aligned} \quad (4.5)$$

Here

$$f_{\mathbf{IP}}(x_{\mathbf{IP}}) = f_{\mathbf{IP}}(x_{\mathbf{IP}}, \mathbf{q} = 0) = \int d^2\mathbf{b} f_{\mathbf{IP}}(x_{\mathbf{IP}}, \mathbf{b}). \quad (4.6)$$

Now, we should make the following replacement in the cross section:

$$\begin{aligned} f_{\mathbf{IP}}(x_{\mathbf{IP},1}) f_{\mathbf{IP}}(x_{\mathbf{IP},2}) &= \int d^2\mathbf{b} d^2\mathbf{b}_1 d^2\mathbf{b}_2 \delta^2(\mathbf{b} - \mathbf{b}_1 + \mathbf{b}_2) \\ &\quad \times f_{\mathbf{IP}}(x_{\mathbf{IP},1}, \mathbf{b}_1) f_{\mathbf{IP}}(x_{\mathbf{IP},2}, \mathbf{b}_2) \\ &\rightarrow \int d^2\mathbf{b} d^2\mathbf{b}_1 d^2\mathbf{b}_2 \delta^2(\mathbf{b} - \mathbf{b}_1 + \mathbf{b}_2) \\ &\quad \times S_{\text{abs}}^2(\mathbf{b}) f_{\mathbf{IP}}(x_{\mathbf{IP},1}, \mathbf{b}_1) f_{\mathbf{IP}}(x_{\mathbf{IP},2}, \mathbf{b}_2). \end{aligned}$$

TABLE I. Survival probability factor for purely exclusive and inclusive double-diffractive processes.

\sqrt{s} [GeV]	$pp \rightarrow p + Z^0 X + p$	$pp \rightarrow Y_1 + Z_0 X + Y_2$
1960	~ 0.05	~ 0.06
14 000	~ 0.025	~ 0.03

The treatment of absorptive corrections is in fact fully analogous to the one required for $\gamma\gamma$ collisions in heavy ion collisions, compare e.g. Eq. (2.2) in Ref. [27].

Using the form (4.5) of the Pomeron-flux, we observe, that the Born-level cross section will be multiplied by the effective survival probability factor

$$\begin{aligned} \overline{S^2}(x_{\mathbf{IP},1}, x_{\mathbf{IP},2}) &= \int d^2\mathbf{b} d^2\mathbf{b}_1 d^2\mathbf{b}_2 S_{\text{abs}}^2(\mathbf{b}) \delta^2(\mathbf{b} - \mathbf{b}_1 + \mathbf{b}_2) \\ &\quad \times t_{\mathbf{IP}}(x_{\mathbf{IP},1}, \mathbf{b}_1) t_{\mathbf{IP}}(x_{\mathbf{IP},2}, \mathbf{b}_2) \\ &= \frac{1}{4\pi B_{12}(x_{\mathbf{IP},1}, x_{\mathbf{IP},2})} \int d^2\mathbf{b} S_{\text{abs}}^2(\mathbf{b}) \\ &\quad \times \exp\left[-\frac{\mathbf{b}^2}{4B_{12}(x_{\mathbf{IP},1}, x_{\mathbf{IP},2})}\right]. \end{aligned} \quad (4.7)$$

Here $B_{12}(x_{\mathbf{IP},1}, x_{\mathbf{IP},2}) = B(x_{\mathbf{IP},1})B(x_{\mathbf{IP},2})/(B(x_{\mathbf{IP},1}) + B(x_{\mathbf{IP},2}))$. In fact, due to the very small Pomeron Regge-slope in the H1-fit the $x_{\mathbf{IP},1} - x_{\mathbf{IP},2}$ dependence can be safely neglected. An admittedly oversimplified two-channel toy model for the absorption factor $S_{\text{abs}}^2(\mathbf{b})$, is described in the Appendix. It yields the numbers given in Table I.

V. RESULTS

Before we go to hadronic reactions let us first present predictions for the $\gamma p \rightarrow Z^0 p$ reaction. In Fig. 6 we show the total cross section as a function of photon-proton center-of-mass energy W . In this calculation we have used the unintegrated gluon distribution from Ref. [15] and the slope parameter B taken from Eq. (2.10). The cross section grows quickly with the energy from the kinematical threshold $W_{\text{th}} = m_Z + m_p$. At typical HERA energy $W = 200$ GeV the cross section is of the order of 10^{-5} nb, i.e. too small to be measured. However, it grows quickly with energy and at $W = 10$ TeV it is already of the order of 1 pb. We show not only the cross section with the full amplitude (including all flavors) but also results with three ($u + d + s$: dotted), four ($u + d + s + c$: dashed) and five ($u + d + s + c + b$: solid) flavors. At low energies it is enough to include only light flavors, while at large energies all flavors must be included.

In Fig. 7 we show distributions in rapidity for the $p\bar{p} \rightarrow p\bar{p}Z^0$ (Tevatron) and $pp \rightarrow ppZ^0$ (LHC) without (black thin solid) and with (grey thick solid) absorption effects. The Born approximation cross section calculated here is much larger than that calculated in the dipole approach in

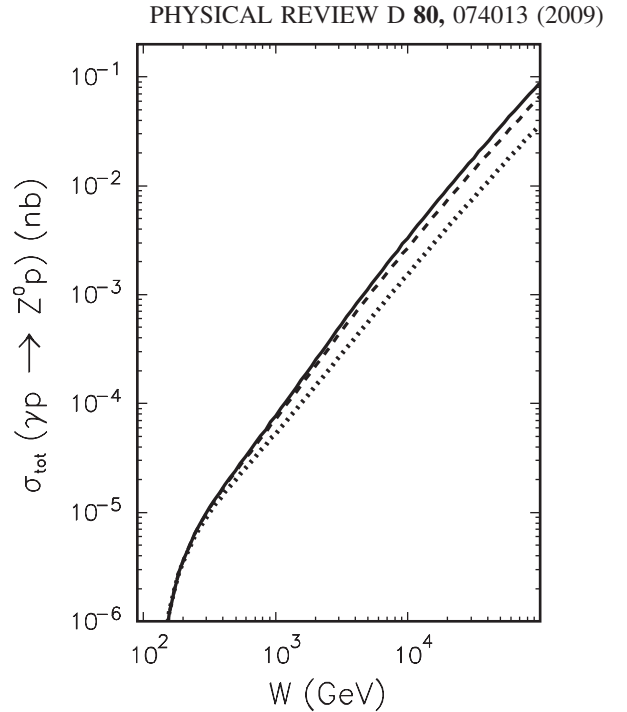


FIG. 6. The total cross section for the $\gamma p \rightarrow Z^0 p$ reaction as a function of photon-proton center-of-mass energy for the Ivanov-Nikolaev unintegrated gluon distribution. The dotted line includes $u + d + s$, the dashed line $u + d + s + c$, and the solid line: $u + d + s + c + b$.

Refs. [7,8]. Generally the absorption effects lower the cross section. The effect depends on the rapidity. Absorptive corrections for exclusive Z^0 production are bigger than for the exclusive production of J/Ψ [5] and Υ [6]. This is due to the fact that for heavy particle production on average higher four-momentum transfers (and hence less peripheral collisions) are involved than for lighter particles. Analogously as for photoproduction $\gamma p \rightarrow Z^0 p$ in Fig. 8 we show the distribution in Z -boson rapidity in the Born approximation calculated with a different number of flavors included in the calculation. While for the Tevatron energy it is enough to include four flavors (u, d, s, c) at the LHC energy five flavors must be included. At the LHC the inclusion of the b quarks increases the cross section by about 20%.

In Fig. 9 we show separate contributions of photon-Pomeron and Pomeron-photon fusion mechanisms as well as the sum of both processes. We wish to stress the fact that in rapidity distributions all interference phenomena disappear if absorption corrections are neglected. At the LHC the two contributions are better separated which leads to the camel-like shape with minimum of the cross section at $y \approx 0$.

The cross sections at the Tevatron energy $\sqrt{s} = 1.96$ TeV is rather small. A recent search for the exclusive Z^0 production [10] has found only an upper limit for this process. There is a hope that at the LHC it could be measurable. One should remember, however, that in prac-

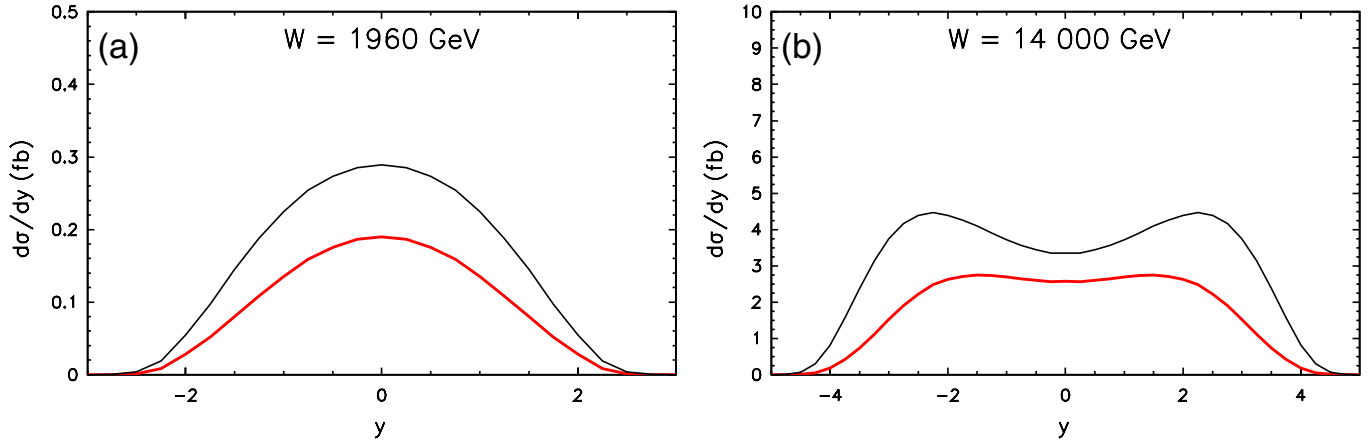


FIG. 7 (color online). Rapidity distribution of the exclusively produced Z^0 for the Tevatron (left) and LHC (right) energies. The black thin solid line corresponds to Born amplitudes and the grey thick solid line (red online) includes absorption effects.

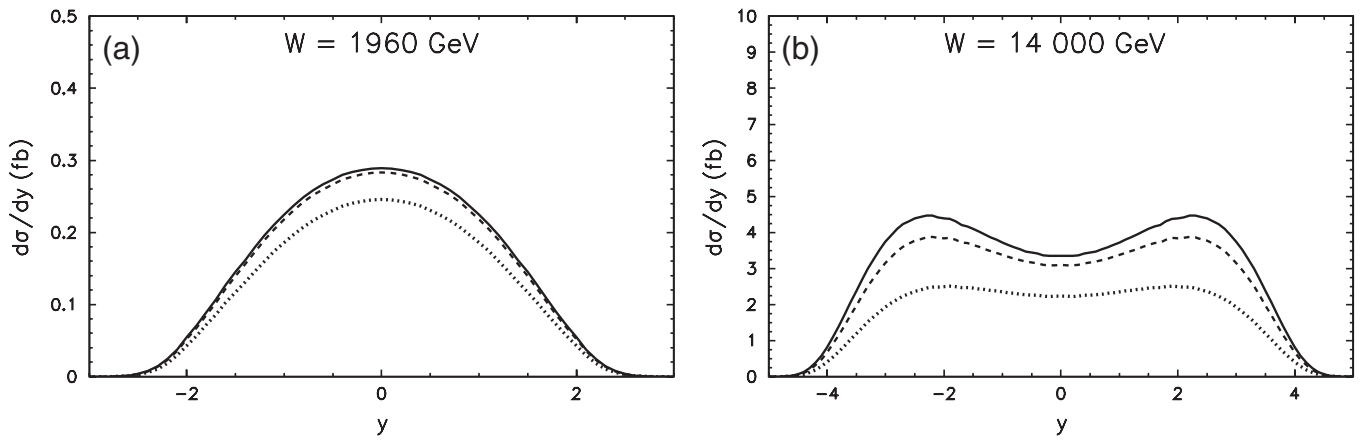


FIG. 8. The influence of different flavors on rapidity distributions of Z^0 for Tevatron (left) and LHC (right) energies. The dotted line includes $u + d + s$, the dashed line $u + d + s + c$, and the solid line: $u + d + s + c + b$.

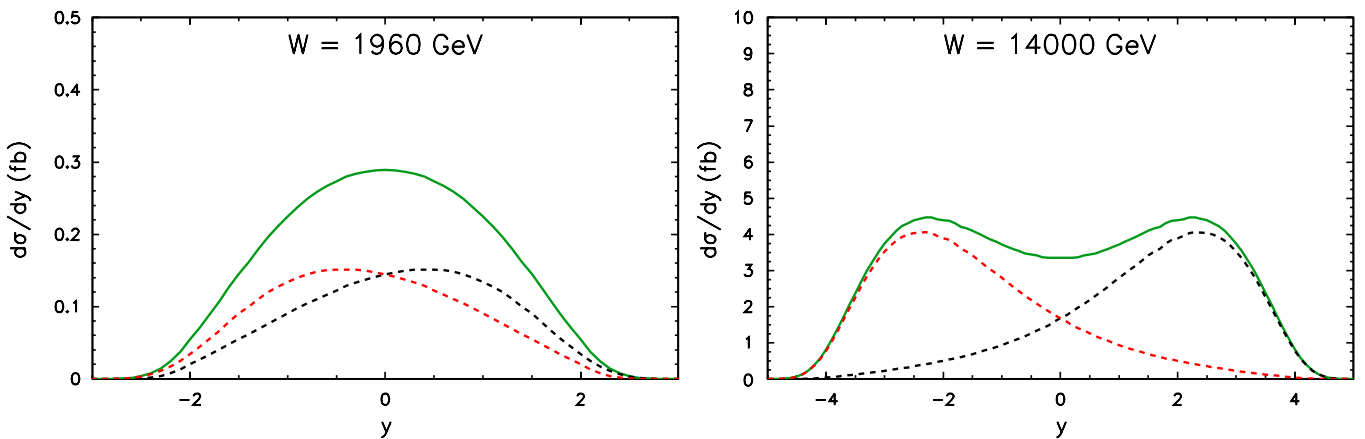


FIG. 9 (color online). The photon-Pomeron and Pomeron-photon contributions for the Tevatron (left) and LHC (right) energies. No absorptive corrections are included here.

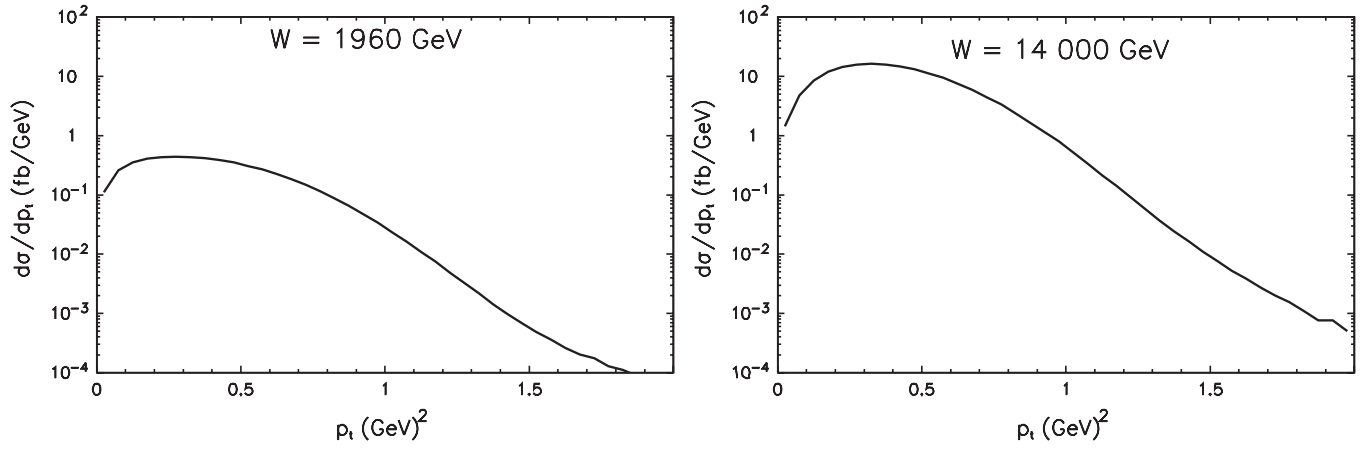


FIG. 10. The transverse momentum distribution of Z^0 bosons at $\sqrt{s} = 1960$ GeV (left) and $\sqrt{s} = 14$ TeV (right).

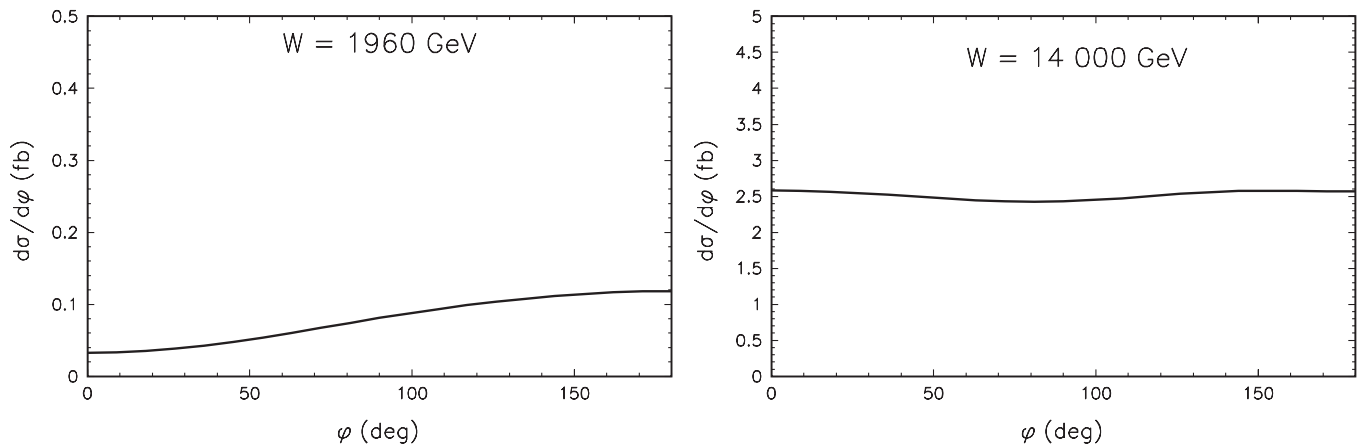


FIG. 11. Distribution in relative azimuthal angle between outgoing protons at $\sqrt{s} = 1960$ GeV (left) and $\sqrt{s} = 14$ TeV (right).

tice one can measure either $\mu^+\mu^-$ or e^+e^- pairs. This means one can expect a sizeable background from the $\gamma^*\gamma^* \rightarrow l^+l^-$ processes [10].² In order to get rid of this type of the background some cuts could be helpful.

In Fig. 10 we show the transverse momentum distribution of the exclusively produced Z^0 . The distribution peaks at $p_t \sim 0.3$ GeV and extends to relatively large transverse momenta. This is in clear contrast to the photon-photon processes where the corresponding transverse momenta of the lepton pair would peak at much lower transverse momenta. We wish to point out, however, that the precise shape of the p_t -distribution depends crucially on the input t -dependence of the $\gamma p \rightarrow Zp$ amplitude, for which we rely on an educated guess. Imposing a lower cut on the lepton pair transverse momenta would cut off the unwanted photon-photon background.

There are definite plans that both ATLAS and CMS main detectors will be supplemented by several forward detec-

tors. In principle, having two forward detectors could allow to measure two outgoing protons in coincidence. This could allow studying correlations between outgoing protons. As an example in Fig. 11 we show the distribution in relative azimuthal angle between outgoing protons. Quite different distributions are obtained for the Tevatron ($\bar{p}p$ collisions) and LHC (pp collisions). This effect is of the interference nature and was already discussed for exclusive J/Ψ production [5]. In contrast to the reaction with the Z^0 boson the relative azimuthal angle distribution for the photon-photon processes peaks sharply at $\phi \sim 180^\circ$ [10]. Therefore imposing extra cuts in the azimuthal angle space should further diminish the photon-photon background opening a chance to measure for the first time the exclusive Z^0 production in proton-proton collisions.

Finally let us present our estimate of the inclusive double-diffractive contribution of Fig. 3. In Fig. 12 we show the cross section with Pomeron exchanges only (dashed) and with both Pomeron and Reggeon exchanges included (solid). These cross sections have to be multiplied in addition by the gap survival probabilities from Table I. In this calculation $x_{\mathbb{P}}^{\max} = 0.1$ was assumed. This means

²Within the standard model, the $\gamma\gamma \rightarrow Z^0$ transition is absent at the tree level. In fact, single- Z^0 production in $\gamma\gamma$ collisions has up to now not been observed experimentally.

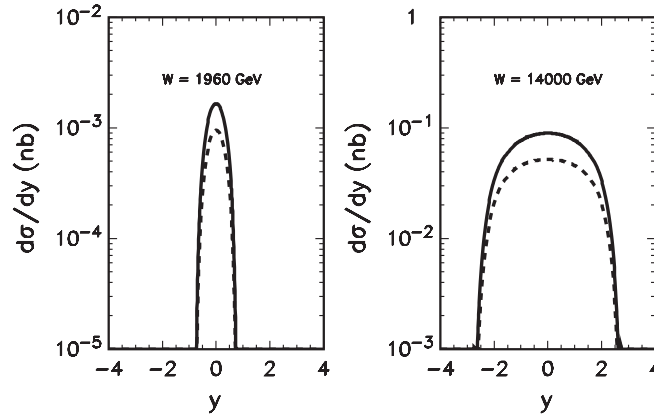


FIG. 12. Rapidity distributions of inclusive double-Pomeron production of Z^0 boson for the Tevatron (left) and LHC (right). The solid lines include both Pomeron and Reggeon exchanges while the dashed lines only Pomeron exchanges. In this calculation the fit (a) from Ref. [21] was used. No absorptive corrections were included here.

cuts on longitudinal momentum fractions of outgoing protons/antiprotons. Even after including absorption corrections the inclusive double-Pomeron contribution is a few orders of magnitude larger than the purely exclusive cross section.

The rapidity distributions from Fig. 12 are more narrow than the purely exclusive distributions shown earlier. This

is partially related to the cuts on longitudinal momentum fractions and is of purely kinematic origin. The cross section for inclusive double-Pomeron contribution is certainly measurable at the LHC and is bigger than the cross section for single-diffractive Z^0 production at the Tevatron [28].

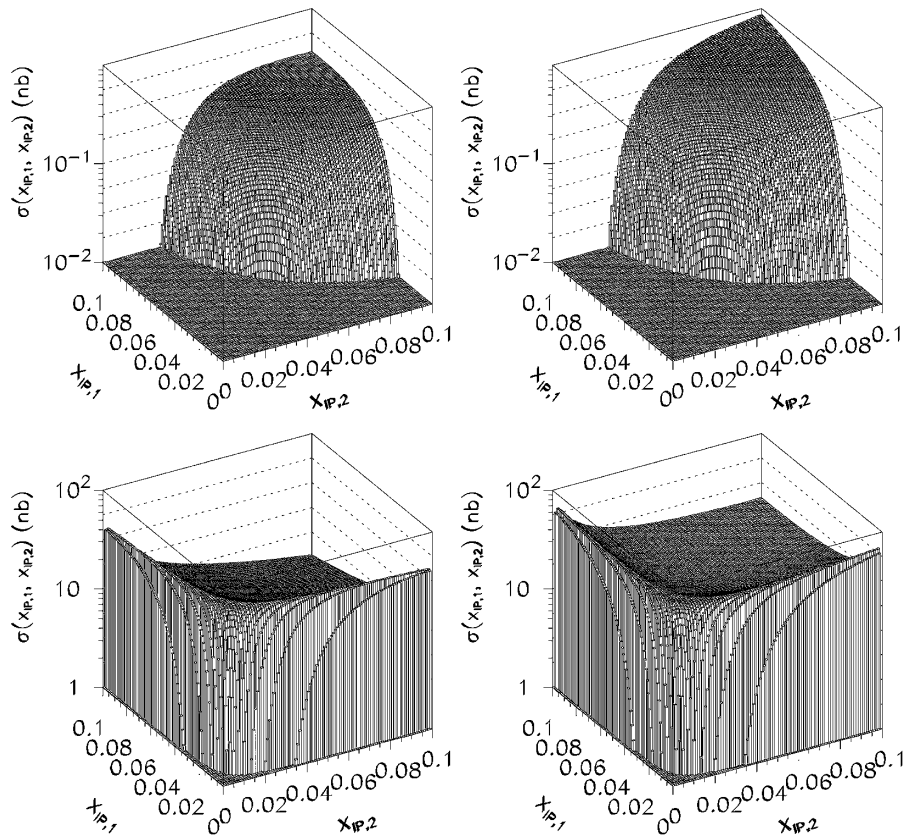


FIG. 13. Two-dimensional distributions in $(x_{IP,1}, x_{IP,2})$ for the Tevatron energy $W = 1960$ GeV (upper panels) and for the LHC energy $W = 14000$ GeV (lower panels). The left panels include only Pomeron exchanges while the right panels both Pomeron and Reggeon exchanges. In this calculation the fit (a) from Ref. [21] was used. No absorption corrections were included here.

In Fig. 13 we show two-dimensional distribution in Pomeron/Reggeon momentum fractions ($x_{\mathbf{IP},1}, x_{\mathbf{IP},2}$). The large mass of the Z^0 boson causes that the small values of $x_{\mathbf{IP},1}$ and $x_{\mathbf{IP},2}$ are not accessible kinematically. This is more evident for the Tevatron energy. This is also the reason for a much smaller cross section for double-diffractive production of Z^0 for the Tevatron compared to the LHC.

VI. CONCLUSIONS

We have extended the k_{\perp} -factorization to the exclusive production of Z^0 bosons. The production amplitude was calculated using an unintegrated gluon distribution [15] adjusted to inclusive deep inelastic structure functions. The so obtained $\gamma p \rightarrow Zp$ amplitude served as an input for the evaluation of the $pp \rightarrow ppZ^0$ process. Our results obtained with bare (i.e., without absorption) amplitudes are by a factor of 3 larger than those obtained earlier in the dipole approach. We have analyzed the role of individual flavors. For low energy it is enough to include only light flavors while at high energies all flavors must be included.

Compared to earlier works in the literature we have taken into account absorption effects. The absorption effects depend on the Z -boson rapidity and lower the cross section by a factor of 1.5–2. As for the exclusive Y production [6] the larger rapidity, the larger the absorption effect.

Very small cross sections are obtained both for the Tevatron and LHC. This means that possible background must be studied. The Z^0 is measured via e^+e^- or $\mu^+\mu^-$ decay channels. Recently the the CDF Collaboration [10] presented a first estimate of the upper limit for the exclusive Z^0 production at the Tevatron. Their limit is about 3 orders of magnitude larger than our predictions. This demonstrates difficulties to measure the exclusive process. The situation will improve at the LHC (larger cross section, larger luminosity), but even there it will be rather difficult to measure the cross section.

In a detailed analysis a background from the $\gamma\gamma \rightarrow l^+l^-$ and $\gamma\mathbf{IP} \rightarrow \gamma^* \rightarrow l^+l^-$ (sub)processes must be taken into account. We have found that distributions in Z^0 (lepton pair) transverse momentum as well as in relative azimuthal angle between outgoing protons can be very useful to separate out the background $\gamma\gamma \rightarrow l^+l^-$ processes.

To our knowledge, for the first time in the literature, we have estimated inclusive double-diffractive production of Z^0 using diffractive parton distributions obtained recently from the analysis of the proton diffractive structure functions/diffractive dijets performed by the H1 Collaboration at HERA. We have estimated cross section assuming Regge-factorization as well as including absorption effects leading to the factorization breaking. Rather large inclusive double-diffractive cross sections were found at the LHC. Future experiments with forward instrumentation of main

LHC detectors (ATLAS and ALICE) should provide new results concerning hard diffraction. This will allow us to further investigate the mechanism of Regge-factorization breaking observed already for soft total single and double diffraction.

ACKNOWLEDGMENTS

We are indebted to Christophe Royon and Laurent Schoeffel for providing us with the H1 parton distributions in the Pomeron. This work was partially supported by the Polish Ministry of Science and Higher Education (MNiSW) under contracts MNiSW N N202 249235 and 1916/B/H03/2008/34.

APPENDIX: TWO-CHANNEL MODEL FOR THE ABSORPTIVE CORRECTIONS

Here we present the details of the two-channel model used for the evaluation of absorptive corrections to central inclusive Z^0 -production. It improves over a single-channel description by taking into account some inelastic shadowing corrections. As physical states, one would include the proton $|p\rangle$ and some effective low-mass states $|N_i^*\rangle$ with proton-quantum numbers (representing e.g. resonances and the diffractively excited $N\pi, N\pi\pi, \dots$ components). The multichannel eikonal will then be an operator acting on the tensor-product space of physical states $|N_i N_j\rangle = |N_i\rangle \otimes |N_j\rangle$, where $N_i = p, N^*$. The proton-proton S -matrix in this space is now given by

$$\hat{S}(\mathbf{b}) = \exp\left[-\frac{1}{2}\nu(s, \mathbf{b})\hat{g} \otimes \hat{g}\right], \quad (\text{A1})$$

where the opacity $\nu(s, \mathbf{b})$ is given by

$$\nu(s, \mathbf{b}) = g_{pp}^2 \left(\frac{s}{s_0}\right)^{\Delta_{\mathbf{IP}}} T_{\mathbf{IP}}(\mathbf{b}), \quad (\text{A2})$$

and we stick to an oversimplified model, in which all matrix elements have the same \mathbf{b} dependence given by $T_{\mathbf{IP}}(\mathbf{b})$. The \mathbf{b} -space profile was taken in the Gaussian form:

$$T_{\mathbf{IP}}(\mathbf{b}) = \frac{1}{2\pi(B_0 + 2\alpha' \log(s/s_0))} \times \exp\left[\frac{-\mathbf{b}^2}{2(B_0 + 2\alpha' \log(s/s_0))}\right]. \quad (\text{A3})$$

The values of the bare Pomeron parameters $g_{pp}^2, \Delta_{\mathbf{IP}}$ as well as the parametrization of $T_{\mathbf{IP}}(\mathbf{b})$ are given below. Notice that below, we do not distinguish between protons and antiprotons, and will always refer to proton-proton scattering even when discussing results for the Tevatron.

In the two-channel case, where all inelastic excitations are subsumed in a single effective state $|N^*\rangle$, the matrix \hat{g} is written as

$$\hat{g} = \begin{pmatrix} 1 + \delta & \gamma \\ \gamma & 1 - \delta \end{pmatrix}. \quad (\text{A4})$$

It has the eigenvalues

$$\lambda_{1,2} = 1 \pm \sqrt{\delta^2 + \gamma^2}, \quad (\text{A5})$$

and the physical states can be expanded into S -matrix eigenstates as

$$|p\rangle = \sum_i C_i^p |i\rangle, \quad |N^*\rangle = \sum_i C_i^{N^*} |i\rangle. \quad (\text{A6})$$

Now we turn to the gap survival probability and evaluate the effective $S_{\text{abs}}^2(\mathbf{b})$ which enters Eq. (4.7). We distinguish different final states.

1. $pp \rightarrow p + Z^0 X + p$

First let us examine the case of the proton-proton final state. Here we need to substitute

$$\begin{aligned} S_{\text{abs}}^2(\mathbf{b}) &\rightarrow |\langle pp | (\hat{g} \otimes \hat{g}) \hat{S}(\mathbf{b}) | pp \rangle|^2 \\ &= |\langle pp | (\hat{g} \otimes \hat{g}) \exp\left[-\frac{1}{2}\nu(s, \mathbf{b}) \hat{g} \otimes \hat{g}\right] | pp \rangle|^2. \end{aligned} \quad (\text{A7})$$

To evaluate the matrix element $\langle pp | \dots | pp \rangle$, we should expand the protons into eigenstates of the S -matrix according to Eq. (A6):

$$\begin{aligned} \langle pp | (\hat{g} \otimes \hat{g}) \hat{S}(\mathbf{b}) | pp \rangle &= |C_1^p|^4 \lambda_1^2 e^{-\nu \lambda_1^2 / 2} + |C_2^p|^4 \lambda_2^2 e^{-\nu \lambda_2^2 / 2} \\ &\quad + 2|C_1^p|^2 |C_2^p|^2 \lambda_1 \lambda_2 e^{-\nu \lambda_1 \lambda_2 / 2}. \end{aligned} \quad (\text{A8})$$

Here we suppressed the arguments of $\nu = \nu(s, \mathbf{b})$.

2. $pp \rightarrow Y_1 + Z^0 X + Y_2$

If protons in the final state cannot be measured, we need to sum over all excitations $Y_{1,2} \in \{p, N^*\}$, and we should substitute

$$\begin{aligned} S_{\text{abs}}^2(\mathbf{b}) &\rightarrow \sum_{Y_1, Y_2} |\langle Y_1 Y_2 | (\hat{g} \otimes \hat{g}) \hat{S}(\mathbf{b}) | pp \rangle|^2 \\ &= \langle pp | (\hat{g} \otimes \hat{g})^2 \hat{S}^2(\mathbf{b}) | pp \rangle \\ &= \langle pp | (\hat{g} \otimes \hat{g})^2 \exp[-\nu(s, \mathbf{b}) \hat{g} \otimes \hat{g}] | pp \rangle \\ &= |C_1^p|^4 \lambda_1^4 e^{-\nu \lambda_1^2} + |C_2^p|^4 \lambda_2^4 e^{-\nu \lambda_2^2} \\ &\quad + 2|C_1^p|^2 |C_2^p|^2 (\lambda_1 \lambda_2)^2 e^{-\nu \lambda_1 \lambda_2}. \end{aligned} \quad (\text{A9})$$

Equivalent equations can be found in [25], which we largely follow in choosing $\gamma = 0.55$, $\delta = 0$. Then

$$|p\rangle = \frac{1}{\sqrt{2}}(|1\rangle + |2\rangle), \quad |N^*\rangle = \frac{1}{\sqrt{2}}(|1\rangle - |2\rangle), \quad (\text{A10})$$

with eigenvalues $\lambda_{1,2} = (1 \pm \gamma)$. The bare Pomeron parameters used in the parametrization of the opacity (A2) with $s_0 = 1 \text{ GeV}^2$, are taken as

$$\begin{aligned} g_{pp}^2 &= 27 \text{ mb}, & \Delta_{\mathbf{P}} &= 0.11, & B_0 &= 9 \text{ GeV}^{-2}, \\ & & \alpha' &= 0.14 \text{ GeV}^{-2}. \end{aligned} \quad (\text{A11})$$

These parameters are adjusted so that we obtain reasonable values for the total cross section σ_{tot} , the elastic cross section σ_{el} , as well as the elastic slope B_{el} . They are obtained from

$$\begin{aligned} \sigma_{\text{tot}} &= 2 \int d^2 \mathbf{b} \Gamma(\mathbf{b}), & \sigma_{\text{el}} &= \int d^2 \mathbf{b} \Gamma^2(\mathbf{b}), \\ B_{\text{el}} &= \frac{1}{2} \frac{\int d^2 \mathbf{b} \mathbf{b}^2 \Gamma(\mathbf{b})}{\int d^2 \mathbf{b} \Gamma(\mathbf{b})}, \end{aligned} \quad (\text{A12})$$

where the impact-parameter space forward amplitude $\Gamma(\mathbf{b})$ is given by

$$\Gamma(\mathbf{b}) = 1 - \langle pp | \hat{S}(\mathbf{b}) | pp \rangle. \quad (\text{A13})$$

For the energy of Tevatron Run I, $\sqrt{s} = 1800 \text{ GeV}$, we obtain $\sigma_{\text{tot}} = 78.5 \text{ mb}$, $\sigma_{\text{el}} = 16.7 \text{ mb}$, and $B_{\text{el}} = 17.2 \text{ GeV}^{-2}$. For the LHC energy of $\sqrt{s} = 14 \text{ TeV}$, this oversimplified model predicts $\sigma_{\text{tot}} = 106 \text{ mb}$, $\sigma_{\text{el}} = 26 \text{ mb}$, and $B_{\text{el}} = 19.8 \text{ GeV}^{-2}$.

-
- [1] T. Aaltonen *et al.* (CDF Collaboration), Phys. Rev. D **77**, 052004 (2008).
 [2] T. Aaltonen *et al.* (CDF Collaboration), Phys. Rev. Lett. **102**, 242001 (2009).
 [3] A.D. Martin, M.G. Ryskin, and V.A. Khoze, arXiv:0903.2980.
 [4] M.G. Albrow *et al.* (FP420 R and D Collaboration), arXiv:0806.0302; R. Schicker, AIP Conf. Proc. **1105**, 136 (2009).
 [5] W. Schäfer and A. Szczurek, Phys. Rev. D **76**, 094014 (2007).
 [6] A. Rybarska, W. Schäfer, and A. Szczurek, Phys. Lett. B **668**, 126 (2008).
 [7] V.P. Goncalves and M.V.T. Machado, Eur. Phys. J. C **56**, 33 (2008).
 [8] L. Motyka and G. Watt, Phys. Rev. D **78**, 014023 (2008).
 [9] I.P. Ivanov, N.N. Nikolaev, and A.A. Savin, Phys. Part. Nucl. **37**, 1 (2006).
 [10] T. Aaltonen *et al.* (CDF Collaboration), Phys. Rev. Lett. **102**, 222002 (2009).
 [11] P. Bruni and G. Ingelman, Phys. Lett. B **311**, 317 (1993); L. Alvero, J.C. Collins, J. Terron, and J.J. Whitmore,

- Phys. Rev. D **59**, 074022 (1999).
- [12] A. G. Shuvaev, K.J. Golec-Biernat, A.D. Martin, and M.G. Ryskin, Phys. Rev. D **60**, 014015 (1999).
- [13] N.N. Nikolaev and B.G. Zakharov, Z. Phys. C **49**, 607 (1991).
- [14] B.Z. Kopeliovich, J. Nemchick, N.N. Nikolaev, and B.G. Zakharov, Phys. Lett. B **309**, 179 (1993).
- [15] I.P. Ivanov and N.N. Nikolaev, Phys. Rev. D **65**, 054004 (2002).
- [16] A. Aktas *et al.* (H1 Collaboration), Eur. Phys. J. C **46**, 585 (2006).
- [17] S. Donnachie, G. Dosch, P. Landshoff, and O. Nachtmann, *Pomeron Physics and QCD* (Cambridge University Press, Cambridge, 2002).
- [18] F. Abe *et al.* (CDF Collaboration), Phys. Rev. D **50**, 5518 (1994).
- [19] G. Ingelman and P.E. Schlein, Phys. Lett. B **152**, 256 (1985).
- [20] V. Barger and R. Phillips, *Collider Physics* (Addison-Wesley Publishing Company, Redwood City, 1987).
- [21] A. Aktas *et al.* (H1 Collaboration), Eur. Phys. J. C **48**, 715 (2006).
- [22] W. Schäfer, in *Deep Inelastic Scattering and QCD: DIS 98: Proceedings* edited by, Gh. Coremans and R. Roosen (World Scientific, Singapore, 1998).
- [23] J.D. Bjorken, Phys. Rev. D **47**, 101 (1993).
- [24] K.A. Ter-Martirosyan, Yad. Fiz. **10**, 1047 (1969) [Sov. J. Nucl. Phys. **10**, 600 (1970)].
- [25] V.A. Khoze, A. D. Martin, and M. G. Ryskin, Eur. Phys. J. C **18**, 167 (2000).
- [26] U. Maor, AIP Conf. Proc. **1105**, 248 (2009).
- [27] M. Klusek, W. Schäfer, and A. Szczurek, Phys. Lett. B **674**, 92 (2009).
- [28] V.M. Abazov *et al.* (D0 Collaboration), Phys. Lett. B **574**, 169 (2003).